*Cerebral Cortex*, December 2015;25: 4885–4897

**doi: 10.1093/cercor/bhv209**
Advance Access Publication Date: 6 October 2015
Original Article

ORIGINAL ARTICLE

# Dopamine D1 Receptor-Mediated Transmission Maintains Information Flow Through the Cortico-Striato-Entopeduncular Direct Pathway to Release Movements

Satomi Chiken[1,2,†], Asako Sato[3,4,†], Chikara Ohta[1,5], Makoto Kurokawa[5], Satoshi Arai[3], Jun Maeshima[3], Tomoko Sunayama-Morita[4,6], Toshikuni Sasaoka[2,3,4,7], and Atsushi Nambu[1,2]

[1]Division of System Neurophysiology, National Institute for Physiological Sciences, Okazaki 444-8585, Japan, [2]School of Life Science, SOKENDAI (The Graduate University for Advanced Studies), Okazaki 444-8585, Japan, [3]Department of Laboratory Animal Science, Kitasato University School of Medicine, Sagamihara 252-0374, Japan, [4]National Institute for Basic Biology, Okazaki 444-8585, Japan, [5]Department of Biological Sciences, Tokyo Metropolitan University, Tokyo 192-0397, Japan, [6]Department of Life Sciences, Graduate School of Arts and Science, The University of Tokyo, Tokyo 153-8902, Japan and [7]Department of Comparative and Experimental Medicine, Brain Research Institute, Niigata University, Niigata 951-8585, Japan

Address correspondence to Atsushi Nambu, Division of System Neurophysiology, National Institute for Physiological Sciences, 38 Nishigonaka, Myodaiji, Okazaki 444-8585, Japan. Email: nambu@nips.ac.jp; Toshikuni Sasaoka, Department of Comparative and Experimental Medicine, Brain Research Institute, Niigata University, Niigata 951-8585, Japan. Email: sasaoka@bri.niigata-u.ac.jp

[†]These authors contributed equally to this work.

## Abstract

In the basal ganglia (BG), dopamine plays a pivotal role in motor control, and dopamine deficiency results in severe motor dysfunctions as seen in Parkinson's disease. According to the well-accepted model of the BG, dopamine activates striatal direct pathway neurons that directly project to the output nuclei of the BG through D1 receptors (D1Rs), whereas dopamine inhibits striatal indirect pathway neurons that project to the external pallidum (GPe) through D2 receptors. To clarify the exact role of dopaminergic transmission via D1Rs in vivo, we developed novel D1R knockdown mice in which D1Rs can be conditionally and reversibly regulated. Suppression of D1R expression by doxycycline treatment decreased spontaneous motor activity and impaired motor ability in the mice. Neuronal activity in the entopeduncular nucleus (EPN), one of the output nuclei of the rodent BG, was recorded in awake conditions to examine the mechanism of motor deficits. Cortically evoked inhibition in the EPN mediated by the cortico-striato-EPN direct pathway was mostly lost during suppression of D1R expression, whereas spontaneous firing rates and patterns remained unchanged. On the other hand, GPe activity changed little. These results suggest that D1R-mediated dopaminergic transmission maintains the information flow through the direct pathway to appropriately release motor actions.

**Key words:** basal ganglia, conditional knockdown, dopamine receptor, extracellular recording, mouse

## Introduction

In the basal ganglia (BG), dopaminergic transmission plays a pivotal role in the control of voluntary movements and motor learning (Albin et al. 1989; DeLong 1990; Gerfen et al. 1990; Graybiel 2005; Joshua et al. 2009; Enomoto et al. 2011). Dopamine deficiency, as occurs in Parkinson's disease (PD), results in severe motor and nonmotor dysfunctions including bradykinesia, rigidity, tremor, autonomic abnormalities, cognitive dysfunction, and depression (Fahn et al. 2011; Seppi et al. 2011). Dopaminergic inputs from the substantia nigra pars compacta terminate in the striatum and are thought to differentially modulate the excitability of 2 types of striatal projection neurons through different receptors (Albin et al. 1989; DeLong 1990; Mallet et al. 2006) (Fig. 1A, left). One is excitatory effects through dopamine D1 receptors (D1Rs) on direct pathway neurons that directly project to the output nuclei of the BG, the entopeduncular nucleus (EPN), which is homologous to the internal segment of the globus pallidus (GPi) in primates, and substantia nigra pars reticulata (SNr). The other is inhibitory effects through D2 receptors (D2Rs) on indirect pathway neurons that project to the external segment of the globus pallidus (GPe), which is also called the globus pallidus in rodents. Such differential effects of dopamine through D1Rs and D2Rs were originally proposed based on changes in gene expression, glucose utilization, and receptor binding in these pathways under conditions of dopamine depletion (Gerfen et al. 1990; Hirsch et al. 2000) and have been reinforced by recent in vitro electrophysiological studies (Surmeier et al. 2007; Day et al. 2008; Flores-Barrera et al. 2011; Gerfen and Surmeier 2011; Planert et al. 2013). The striato-EPN/SNr direct and striato-GPe-subthalamo (STN)-EPN/SNr indirect pathways play opposite roles in controlling movements. The signals through the direct pathway reduce activity of the EPN/SNr and increase thalamocortical activity via disinhibition, resulting in release of movements. In contrast, signals through the indirect pathway increase activity of the EPN/SNr, resulting in suppression of movements (Albin et al. 1989; DeLong 1990; Gerfen et al. 1990; Mink 1996; Nambu 2007; Kravitz et al. 2010; Sano et al. 2013). Thus, the loss of dopaminergic inputs to both pathway neurons is considered to increase firing rates of EPN/SNr neurons through the inhibitory striato-EPN/SNr direct and net excitatory

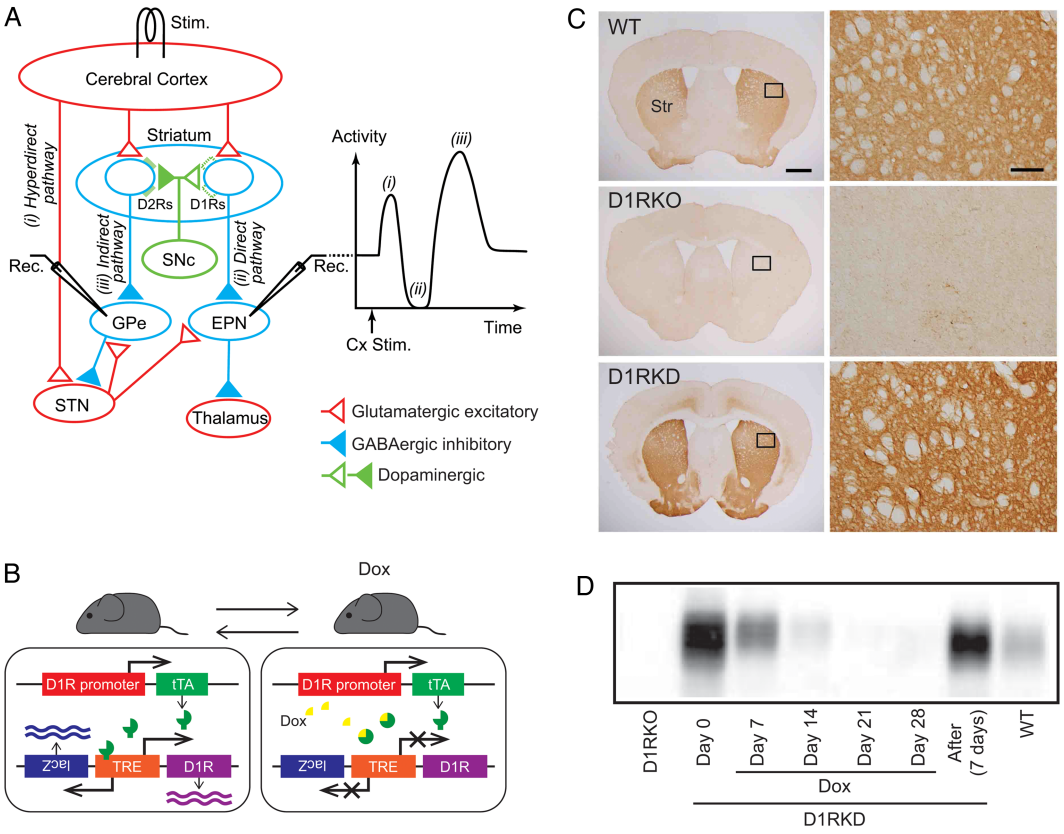


**Figure 1.** Dopamine D1 receptor (D1R) suppression in D1R knockdown (D1RKD) mice with doxycycline (Dox) treatment. (*A*) Schematic diagram showing the cortico-basal ganglia pathway and stimulating (Stim.) and recording (Rec.) sites in the electrophysiological experiments (left), along with a typical response pattern (right) in the entopeduncular nucleus (EPN) (homologous to the internal segment of the globus pallidus, GPi) to cortical stimulation (Cx Stim.) with early excitation, inhibition, and late excitation, which are mediated by the i) cortico-subthalamo (STN)-EPN hyperdirect, ii) cortico-striato-EPN direct, and iii) cortico-striato-external pallido (GPe)-STN-EPN indirect pathways, respectively. Red, blue, and green triangles represent glutamatergic excitatory, GABAergic inhibitory, and dopaminergic projections, respectively. D2Rs, dopamine D2 receptors; SNc, substantia nigra pars compacta. (*B*) Schematic diagram of Dox-regulated D1R expression in D1RKD mice. Before Dox treatment (left), tetracycline transactivator (tTA) binds to the tetracycline responsive element (TRE), and D1Rs and lacZ are transcribed. Dox treatment interferes with tTA binding to TRE (right), and suppresses D1R and lacZ expression (Tet-off system). (*C*) D1R immunoreactivity in the striatum (Str) of wild-type (WT, top), D1R knockout (D1RKO, middle), and D1RKD (before Dox treatment, bottom) mice shown in frontal sections. The pattern of D1R expression in D1RKD mice was similar to that in WT mice, whereas D1R immunoreactivity was not observed in D1RKO mice. The dorsolateral motor areas of the Str are defined by rectangles (left) and shown at higher magnification (right). Scale bars, 1 mm on the left, 100 μm on the right. (*D*) Western blot analysis of D1R protein expression in the striatum of a D1RKO mouse ($n = 1$, number of mice used), D1RKD mice before, during, and after Dox treatment (Days 0, 7, 14, 21, 28, different days after starting Dox treatment; After, 7 days after cessation of Dox treatment for 14 days; $n = 3$–4 per condition), and WT mice ($n = 3$).

striato-GPe-STN-EPN/SNr indirect pathways, resulting in the decreased motor activity seen in PD (Albin et al. 1989; DeLong 1990).

However, the exact role of D1R-mediated dopaminergic transmission in vivo is not well understood. Contradicting results have been observed following D1R blockade. D1R knockout (KO) mice show increases in spontaneous locomotor activity, although pharmacological blockade of D1Rs induces locomotor suppression in agreement with the above explanation (Waddington et al. 2005). In the present study, we developed novel D1R knockdown (D1RKD) mice in which the D1Rs can be conditionally and reversibly regulated by doxycycline (Dox) treatment (Fig. 1*B*). The D1RKD mice enabled us to examine motor behaviors and neuronal activities in the cortico-BG pathways in the presence and absence of D1Rs in the same mice. The mice exhibited decreased spontaneous motor activity and impaired motor ability when D1R expression was suppressed, consistent with the pharmacological blockade study (Waddington et al. 2005). To examine the neural mechanism of the motor deficits, we next recorded neuronal activity in the EPN in awake mice, because the EPN is the main output nucleus of the BG to the thalamus and the target of D1R-expressing striatal neurons. Cortically evoked inhibition in the EPN, which is mediated by the cortico-striato-EPN direct pathway, was mostly lost during suppression of D1R expression, whereas spontaneous firing rates and patterns of EPN neurons remained unchanged. These results indicate that D1R suppression mostly blocks the information flow through the cortico-striato-EPN direct pathway and reduces spontaneous motor activity.

## Materials and Methods

Animal protocols were approved by the Institutional Animal Care and Use Committee of National Institutes of Natural Sciences, Kitasato University and Niigata University, and were conducted according to the guidelines of the National Institutes of Health *Guide for the Care and Use of Laboratory Animals*. One to 5 mice were housed in each cage under a 12-h light–dark cycle (lights on at 8:00 AM) and given food and drinking water *ad libitum*.

### Generation of Conditional and Reversible D1RKD Mice

We developed D1RKD mice in which D1Rs can be conditionally and reversibly regulated by Dox using the Tet-Off system after deletion of the endogenous D1Rs (Fig. 1*B*). To generate tetracycline transactivator-VP16 (tTA)-expressing mice using the *D1R* promoter (transactivator line), bacterial artificial chromosome (BAC) clones containing mouse *D1R* were modified with a 2-step Rec A strategy for BAC modification (Yang et al. 1997). A modification cassette that introduces the tTA into the endogenous *D1R* coding sequence was constructed (see Supplementary Fig. 1*A*). A DNA fragment (0.92 kb, A-arm) containing the upstream region of the translation initiation site of *D1R* was ligated to the DNA fragment (1.5 kb) containing the coding sequence of the tTA and the SV40 poly A signal (poly A) of the pTet-off vector (Clontech), and the resulting fragment was ligated to the DNA fragment (0.96 kb, B-arm) of exon 2 of *D1R* to generate D1Txx, the modification cassette (3.38 kb). Because the tTA and the SV40 poly A signal sequences were introduced at the initiation codon of *D1R*, the expression of endogenous *D1R* was disrupted. To generate the pSV1-RecA-D1T shuttle vector, the DNA fragment of D1Txx was inserted into the pSV1-RecA vector to facilitate homologous recombination in RecA$^-$ *Escherichia coli*.

The BAC clone, BAC4-D1R (80 230 bp) (Research Genetics), was used (see Supplementary Fig. 1*B*). RecA$^-$ *E. coli* carrying the original BAC clone were transformed with the pSV1-RecA-D1T shuttle vector. The resulting clones were subjected to Southern analysis using either a 5′ probe or tTA probe to confirm proper recombination (see Supplementary Fig. 1*A*). The BAC transgenic (Tg) construct, BAC4-tTA, was obtained (see Supplementary Fig. 1*B*).

The Tg construct, D1R-tetracycline responsive element (D1R-TRE), was generated for tetracycline operator (tetO)-target Tg mouse lines using the following DNA fragments (see Supplementary Fig. 1*C*): a 9.7-kb fragment including the entire *D1R* coding sequence, a 0.64-kb fragment encoding the TRE and bidirectional promoter from the pBI Tet vector (Clontech), a 3466-bp fragment encoding *lacZ* from the pBI-GL Tet vector (Clontech), a 0.98-kb fragment containing rabbit beta-globin poly A and SV40 poly A signals from the pBstN plasmid, and a 0.3-kb fragment encoding the chicken beta-globin insulator sequences from the plasmid pUC19 INS240-SNNS.

The BAC4-tTA and D1R-TRE DNAs (10 ng/μL each) were used for Tg mouse generation using standard techniques (Nagy et al. 2002). The BAC4-tTA and D1R-TRE DNAs were independently microinjected into fertilized mouse oocytes isolated from crosses of D1R homozygous knockout (D1RKO) female and male mice (Tran et al. 2008). Three Tg lines for BAC4-tTA and 15 Tg lines for D1R-TRE were independently generated. Each BAC4-tTA Tg line was crossed with each D1R-TRE Tg line. The progeny from crosses of BAC4-tTA and D1R-TRE Tg mice was subjected to analyses of Dox-controllable expression of *lacZ* using X-gal staining of brain sections using a standard method and expression of D1R in the striatum using western blotting with anti-D1R antibody (Sigma). Two Tg lines harboring BAC4-tTA and D1R-TRE (designated 442–43 and 442–112) were consistently found to exhibit distinct, comparable expression of *lacZ* in the region where endogenous *D1R* was expressed and Dox-controllable expression of *lacZ* and *D1R*. Therefore, the 442–112 line was used for further analyses as D1RKD mice.

Wild-type (WT) C57BL/6J and D1RKO (Tran et al. 2008) mice were also used for comparison in immunohistochemical, western blot, and behavioral analyses.

### Dox Treatment

Dox (2.0 mg/mL) was mixed in drinking water containing 5% sucrose and delivered to the D1RKD and WT mice through a water bottle.

### Immunohistochemistry

We used 4 D1RKD, 3 WT, and 1 D1RKO mice for immunohistochemical analysis. Mice were deeply anesthetized by injection of tribromoethanol (400 mg/kg body weight, i.p.) and perfused transcardially with 4% paraformaldehyde in phosphate buffer (PB, pH 7.4). The brains were postfixed overnight at 4°C, transferred to a 30% sucrose solution, immersed in OCT compound (Sakura Finetek), frozen, and stored at –80°C until use. Frontal sections were cut at 25-μm thickness and stored in PBS at 4°C. Free-floating sections were incubated with 1% bovine serum albumin containing antibody for D1R (1:1000; Frontier Institute) overnight at 4°C. D1R antibody binding was visualized using the Vectastain Elite ABC System (Vector Laboratories) and 3, 3′-diaminobenzidine.

### Western Blot Analysis

We used 19 D1RKD (3–4 in each condition, 0, 7, 14, 21, and 28 days after starting Dox treatment and 7 days after cessation of Dox treatment for 14 days), 3 WT, and 1 D1RKO mice for western

blot analysis as described previously (Tran et al. 2008) with minor modifications. Briefly, after euthanasia by cervical dislocation, the striatum was dissected and homogenized in lysis buffer. Total lysates were resolved with 10% SDS-PAGE and transferred to a polyvinylidene difluoride membrane (Millipore). The membrane was blocked with 5% skim milk and incubated with anti-D1R (1:5000; Sigma) or anti-actin (as a protein loading control; 1:500; Sigma) antibodies, followed by incubation with secondary antibodies conjugated to horseradish peroxidase (Sigma). Signals were developed with an ECL detection kit (GE Healthcare). The density of the bands was determined with CS Analyzer software (Atto).

## Behavioral Analyses

D1RKD and age-matched WT male mice (7–28 weeks old) were used for behavioral analyses. D1RKD and WT mice were randomly divided into Dox-treated and untreated groups. All behavioral data are presented as the mean ± SD.

### *Spontaneous Motor Activity*

We assessed spontaneous motor activity of 9 Dox-treated D1RKD, 4 untreated D1RKD, and 5 Dox-treated WT mice. The mice were individually housed in an 11.8 cm (L) × 20.8 cm (W) × 14.5 cm (H) home cage, and movements of each mouse were detected before, during, and after Dox treatment with a pyroelectric infrared sensor installed above the cage (O'hara) as reported previously (Nakamura et al. 2014). Movements were continuously counted in 10-min bins, and spontaneous motor activity per day was calculated as the cumulative number of movements in 24 h beginning at 8:00 AM. The bedding was replaced every 7 days, and motor activity was increased after bedding replacement because of exploratory behavior. Thus, data on these days were excluded when calculating the mean weekly spontaneous motor activity. Spontaneous motor activity was classified into 3 levels based on counts per 10 min: inactive (≤9), low (10–199), and high (≥200). We also assessed spontaneous motor activity of another 4 Dox-treated D1RKD and 4 Dox-treated WT mice until 10 days after cessation of Dox treatment for 14 days.

### *Rotarod Test*

We used another 13 Dox-treated D1RKD, 5 untreated D1RKD, 8 Dox-treated WT, and 15 untreated WT mice for the rotarod test. Dox treatment was started 35 days before the test and continued during the test periods for Dox-treated groups. Mice were placed on a rotating rod (32 mm diameter, O'hara), which initially rotated at 4 rpm, and then was accelerated at a constant rate from 4 to 40 rpm over 4 min, with the final speed maintained for 1 min. The time spent on the rotarod was measured in 3 trials every day between 1:00 PM and 7:00 PM and averaged.

## Electrophysiology

### *Surgery*

We used 4 D1RKD (mouse W, K, T, and O, 20–50 weeks old, males) and 3 age-matched WT mice for the electrophysiological experiments. Under anesthesia with ketamine hydrochloride (100 mg/kg, i.p.) and xylazine hydrochloride (4–5 mg/kg, i.p.), a small U-frame polyacetal head holder was fixed to the exposed skull of the mouse with transparent acrylic resin (for details, see Chiken et al. 2008; Sano et al. 2013). After recovery from the first surgery, under light anesthesia with ketamine hydrochloride (30–50 mg/kg, i.p.), a portion of the skull was removed to access the motor cortex, EPN, and GPe. Two pairs of bipolar stimulating electrodes were chronically implanted into the caudal forelimb and orofacial regions of the motor cortex (for details, see Chiken et al. 2008).

### *Recording of Neuronal Activity in the Awake State*

After full recovery from the second surgery, neuronal recording was started (for details, see Chiken et al. 2008; Sano et al. 2013). The awake mouse was kept quiet in a stereotaxic apparatus with its head restrained painlessly using the U-frame head holder. A glass-coated Elgiloy-alloy microelectrode was inserted vertically into the EPN/GPe through the dura mater. Unit activity was isolated and converted to digital pulses using a window discriminator. Spontaneous discharges and responses to the cortical stimulation (200-μs duration, single pulse, 50-μA strength) through the electrodes implanted in the motor cortex were recorded in the EPN/GPe from the same mouse in 3 conditions: before, during, and after Dox treatment. We first recorded neuronal activity before Dox treatment ("before" condition) and then started Dox treatment. Recording of neuronal activity was resumed 5 days after starting Dox treatment and continued till 22 days after starting Dox treatment ("during Dox" condition) when D1R expression was greatly suppressed and spontaneous motor activity was distinctly decreased (Figs 1*D*, 2*A*). Finally, we stopped Dox treatment and resumed recording 15 days after cessation of Dox treatment ("after" condition) when D1R expression and spontaneous motor activity had fully returned to the level prior to Dox treatment (Figs 1*D* and 2*C*). During the recording session, we carefully monitored vigilance state of the mouse by visual inspection.

### *Histology*

In the final experiment, several sites of neuronal recording were marked by passing cathodal DC current (20 μA for 30 s) through the recording electrodes. The mice were anesthetized deeply with sodium pentobarbital (120 mg/kg, i.p.) and perfused transcardially with 0.1 M PB (pH 7.3) followed by 10% formalin in 0.1 M PB, and then 0.1 M PB containing 10% sucrose. The brains were removed immediately and saturated with the same buffer containing 30% sucrose. They were cut into frontal 50-μm-thick sections on a freezing microtome. The sections were mounted onto gelatin-coated glass slides, stained with 0.7% neutral red, dehydrated, and coverslipped. The sections were observed under a light microscope, and the recording sites were reconstructed according to the lesions made by current injection and traces of electrode tracks. The sites of stimulation in the motor cortex were also examined histologically.

### *Data Analysis*

Spontaneous discharge rates were calculated from continuous digitized recordings for 50 s. The following parameters characterizing firing patterns were calculated from the first 30 s of the same recordings: the coefficient of variation (CV) of interspike intervals (ISIs), the burst index (Hutchison et al. 1998; Sano et al. 2013), and the percentage of spikes in bursts detected by the Poisson surprise method (Legéndy and Salcman 1985; Chiken et al. 2008; Sano et al. 2013) (Poisson surprise value ($-\log_{10} P$) ≥2.0; the minimum number of spikes during bursts was 3). Autocorrelograms (bin width of 0.5 ms) were constructed from continuous digitized recordings for 50 s.

Responses to cortical stimulation were examined by constructing peristimulus time histograms (PSTHs; bin width of 1 ms) for 100 stimulus trials. The mean value and SD of the discharge rate during the 100-ms period preceding the stimulation onset were calculated for each PSTH and considered as the

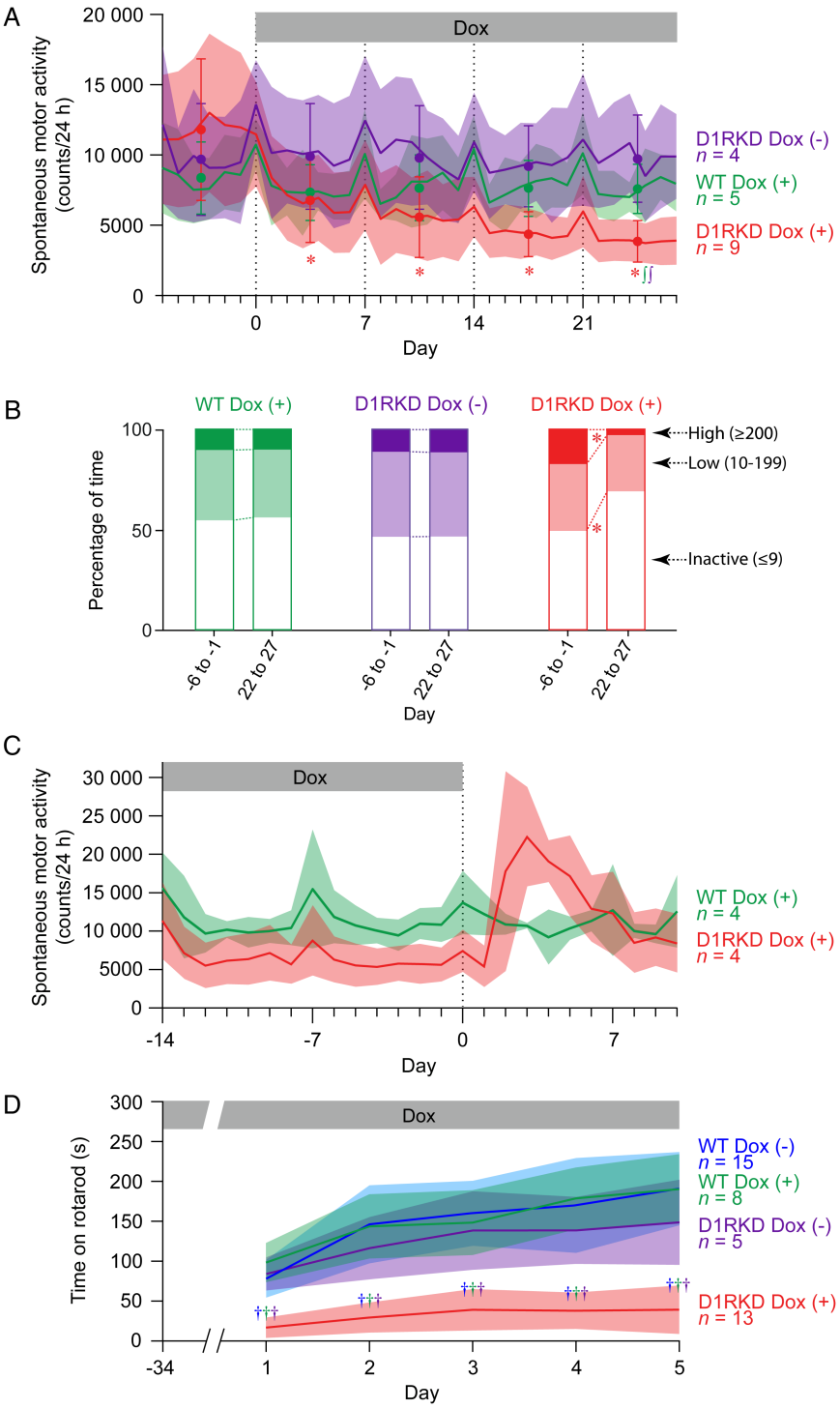


**Figure 2.** Spontaneous motor activity and rotarod performance during D1R suppression. (*A*) Spontaneous motor activity of Dox-treated D1RKD (D1RKD Dox (+)), untreated D1RKD (D1RKD Dox (–)), and Dox-treated WT (WT Dox (+)) mice in their home cages. Dox treatment was started on Day 0 and continued for 4 weeks for Dox-treated groups (gray bar). Daily changes in spontaneous motor activity during Dox treatment were observed. Bedding was replaced every 7 days (Days 0, 7, 14, and 21), and spontaneous motor activity was increased because of exploratory behavior. Thus, data on these days were excluded from further analyses. Colored lines and light-colored areas represent mean and ± SD, and filled circles and whiskers represent mean weekly spontaneous motor activity and ±SD. *$P < 0.05$; significantly different from before Dox treatment (Bonferroni test). $\int P < 0.05$, significantly different from control (WT Dox (+) and D1RKD Dox (–) mice), which is indicated by the corresponding color (Bonferroni test). (*B*) Classifications of spontaneous motor activity of WT Dox (+), D1RKD Dox (–), and D1RKD Dox (+) mice before (Days –6 to –1) and during (Days 22–27) Dox treatment. Spontaneous motor activity was classified into 3 levels based on counts per 10 min: inactive (≤9), low (10–199), and high (≥200). *, the percentage of inactive (≤9) time significantly increased ($\chi^2$ test with Bonferroni correction, $P = 0.008$), and that of high-active (≥200) time significantly decreased ($P = 0.0004$). (*C*) Spontaneous motor activity of D1RKD Dox (+) and WT Dox (+) mice after cessation of Dox treatment. The 2-week Dox treatment was stopped on Day 0. Bedding was replaced every 7 days (Days –14, –7, 0, and 7). (*D*) Rotarod performance of D1RKD Dox (+), D1RKD Dox (–), WT Dox (+), and untreated WT (WT Dox (–)) mice. Dox treatment was started 35 days before the rotarod test. $^{\dagger}P < 0.01$, significantly different from control, which is indicated by the corresponding color (Bonferroni test). The number of mice used for each experiment is indicated by *n*.

baseline discharge rate. Changes in neuronal activity in response to cortical stimulation were judged significant if the discharge rate during at least 2 consecutive bins (2 ms) reached a significance level of $P < 0.05$ (Nambu et al. 2000; Chiken et al. 2008; Tachibana et al. 2008; Sano et al. 2013). The latency of each response was defined as the time at which the first bin exceeded this level. The responses were judged to end when 2 consecutive bins fell below the significance level. The end point was determined as the time at which the last bin exceeded this level. The amplitude of each component of cortically evoked responses was defined as the number of spikes during the significant response minus that of the baseline discharge in the PSTH (i.e., the area of the response; positive and negative values indicate excitation and inhibition, respectively). If no significant changes were found, the amplitude was set to zero. For population PSTHs, the PSTH of each neuron with a significant response was averaged and filtered with a Gaussian filter ($\sigma = 1.6$ ms). All electrophysiological data are presented as the mean ± SD.

## Results

### Biochemical Characteristics of D1RKD Mice

We developed D1RKD mice in which D1Rs were conditionally and reversibly regulated by Dox using the Tet-Off system (Fig. 1*B*, see also Materials and Methods). We first examined the distribution of D1Rs in D1RKD mice immunohistochemically (Fig. 1*C*) using D1R antibodies. The specificity of the antibodies was examined in WT C57BL/6J mice and D1RKO mice (Fig. 1*C*, WT and D1RKO). D1Rs were expressed at a high level in the striatum including the ventral striatum and at moderate levels in the cortex of D1RKD mice (Fig. 1*C*, D1RKD). The distribution of D1Rs was similar to that of WT mice (Fig. 1*C*, WT) and that reported previously (Fremeau et al. 1991; Weiner et al. 1991; Gaspar et al. 1995). We next quantitatively evaluated D1R expression in the striatum of D1RKD mice before, during, and after Dox treatment using western blot analysis (Fig. 1*D*). Before Dox treatment, D1R expression in the striatum was 27-fold higher than that in WT mice (Fig. 1*D*, Day 0 of D1RKD and WT). Dox treatment rapidly and completely suppressed D1R expression (Day 7, 27.1 ± 4.2%; Day 14, 3.1 ± 1.4%; Days 21 and 28, undetectable). After cessation of Dox treatment, D1R expression recovered to the level prior to Dox treatment over 7 days (Fig. 1*D*, After).

### Motor Behaviors During D1R Suppression

Before Dox treatment, D1RKD mice showed normal behaviors and similar spontaneous motor activity to WT mice (Days −6 to −1 in Fig. 2*A*), despite the higher D1R expression in D1RKD mice. Dox treatment significantly decreased spontaneous motor activity in D1RKD mice from the first week (Days 1–6 of D1RKD Dox (+) in Fig. 2*A*) and monotonically decreased their activity during the second, third, and fourth weeks. Dox had little effect on WT mice (WT Dox (+)), and spontaneous motor activity in untreated D1RKD mice (D1RKD Dox (−)) was also unchanged (repeated-measures 2-way ANOVA, $P = 0.0024$ for genotype–day interaction; Bonferroni test, $P = 0.013$ for Days 1–6, $P < 0.01$ for Days 8–13, 15–20 and 22–27). Finally, the difference in the spontaneous motor activity of D1RKD Dox (+) mice and that of WT Dox (+) and D1RKD Dox (−) mice became significant in the fourth week (Days 22–27) (Bonferroni test, $P < 0.01$). Decreased spontaneous motor activity in D1RKD Dox (+) mice was due to an increase in inactive time and a decrease in highly active time (Fig. 2*B*; $\chi^2$ test with Bonferroni correction, $P = 0.008$); such changes in active and inactive times were observed in neither WT Dox (+) nor D1RKD Dox (−) mice. After cessation of Dox treatment, spontaneous motor activity temporarily increased and then returned to the normal level over 7 days (Fig. 2*C*).

Motor ability was also impaired during Dox treatment as evidenced by the rotarod test. The time spent on the rotarod by D1RKD Dox (+) mice was significantly shorter than that for WT Dox (−), WT Dox (+), and D1RKD Dox (−) mice (Fig. 2*D*; repeated-measures 2-way ANOVA, $P < 0.0001$ for genotype–day interaction; Bonferroni test, $P < 0.01$).

### Spontaneous Activity of EPN and GPe Neurons During D1R Suppression

To assess the mechanism of the decreased motor activity in D1RKD mice following D1R suppression, we examined neuronal activity in awake conditions in the motor-related area of the EPN (Chiken et al. 2008), which is the target of D1R-expressing striatal neurons and the main output nucleus of the BG to the thalamus (Fig. 1*A*). We first recorded spontaneous activity of 127 and 89 EPN neurons before and during Dox treatment, respectively, in 4 awake D1RKD mice. EPN neurons continuously and irregularly fired at a high discharge rate (53.9 ± 14.8 Hz) before Dox treatment (Table 1, Fig. 3*A*1) as observed in WT mice (Chiken et al. 2008). Dox treatment did not change either the firing rate (54.2 ± 13.5 Hz; Table 1; 1-way ANOVA, $P = 0.93$) or pattern (Table 1, Fig. 3*A*2). The CV of ISIs, the burst index, and percentage of spikes in bursts, which characterize firing patterns, also did not change. These results indicate that D1R suppression had little influence on the spontaneous activity of EPN neurons. More than 15 days after the cessation of Dox treatment, we recorded 36 EPN neurons and found that the firing rates and percentage of spikes in bursts remained unchanged, whereas the CV of ISIs and burst index were increased (Table 1; 1-way ANOVA with Tukey's post hoc test, $P < 0.001$ for the CV of ISIs and burst index).

For comparison, we also examined the activity of GPe neurons in the same 4 D1RKD mice, because striato-GPe neurons are assumed to express D2Rs, not D1Rs (Fig. 1*A*). We found no significant differences in the firing rate or pattern among the 3 conditions (Table 1; 1-way ANOVA, $P = 0.84$ for the firing rate,

**Table 1** Spontaneous firing rates and patterns of EPN and GPe neurons before, during, and after Dox treatment in D1RKD mice

| | Before | During Dox (5–22 days after starting Dox treatment) | After |
|---|---|---|---|
| EPN | | | |
| No. of neurons | 127 | 89 | 36 |
| Firing rate (Hz) | 53.9 ± 14.8 | 54.2 ± 13.5 | 53.8 ± 19.0 |
| CV of ISIs | 0.53 ± 0.15* | 0.49 ± 0.15# | 0.65 ± 0.19*,# |
| Burst index | 1.33 ± 0.36* | 1.23 ± 0.30# | 1.91 ± 1.19*,# |
| Spikes in bursts (%) | 0.82 ± 2.02 | 0.69 ± 1.27 | 1.16 ± 1.70 |
| GPe | | | |
| No. of neurons | 120 | 100 | 38 |
| Firing rate (Hz) | 51.0 ± 15.8 | 51.1 ± 15.5 | 52.9 ± 16.4 |
| CV of ISIs | 0.63 ± 0.21 | 0.68 ± 0.24 | 0.69 ± 0.15 |
| Burst index | 1.61 ± 1.08 | 1.54 ± 0.47 | 1.69 ± 0.43 |
| Spikes in bursts (%) | 1.43 ± 3.17 | 1.12 ± 1.66 | 1.33 ± 1.80 |

*,#$P < 0.01$, significantly different from each other (1-way ANOVA with Tukey's post hoc test).

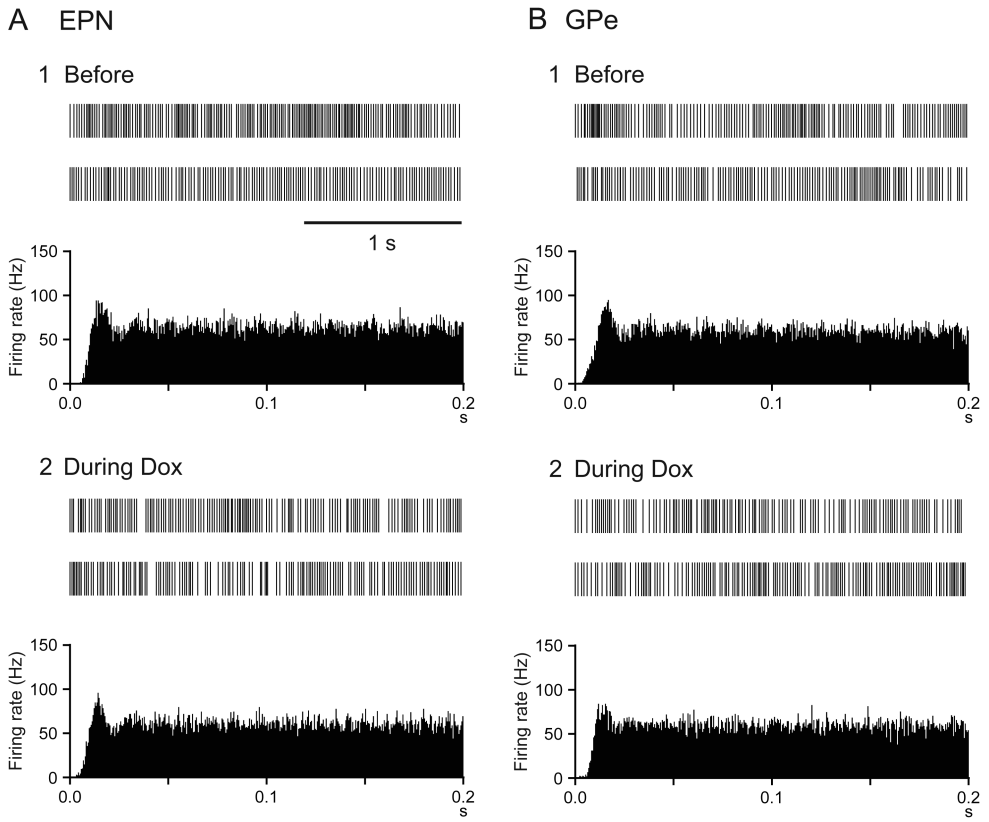


**Figure 3.** Spontaneous activity of EPN and GPe neurons during D1R suppression. Digitized spikes (top) and autocorrelograms (bottom) of spontaneous activity of EPN (*A*) and GPe (*B*) neurons before (*1*) and during (*2*) Dox treatment in D1RKD mice are shown.

$P = 0.26$ for the CV of ISIs, $P = 0.69$ for the burst index, $P = 0.73$ for the percentage of spikes in bursts; Fig. 3*B*).

## Cortically Evoked Responses of EPN and GPe Neurons During D1R Suppression

After recording spontaneous activity of EPN neurons, we next examined the responses of these neurons to electrical stimulation of the forelimb and orofacial regions of the motor cortex (Chiken et al. 2008) (Fig. 4A), because cortical stimulation induces neuronal activity in the BG and mimics information processing during voluntary movements (Chiken et al. 2008; Tachibana et al. 2008; Sano et al. 2013). Before Dox treatment, 60% of EPN neurons (75/125 cells, Table 2) responded to stimulation of the motor cortex. The most common (64%) response was a triphasic response composed of early excitation, followed by inhibition and late excitation (ex-inh-ex) as observed in PSTHs (Fig. 4A1, left, see Supplementary Fig. 2A, Before), which is the typical response in WT mice (Chiken et al. 2008, see also Supplementary Fig. 3B). During Dox treatment, a similar percentage of neurons (72%, 63/88 cells, Table 2) responded to the motor cortical stimulation in the same area of the EPN (Fig. 5A); however, response patterns drastically changed. The inhibition was mostly lost (Fig. 4A2, left). The most common (65%) response was biphasic excitation consisting of early and late excitation, and the percentage of neurons exhibiting responses with inhibition, such as ex-inh-ex, ex-inh, inh-ex, and inh, was significantly decreased (before, 84%; during Dox, 24%; $\chi^2$ test, $P < 0.0001$, see Supplementary Fig. 2A). These changes were also clearly observed in population PSTHs. The inhibition disappeared during Dox treatment (Fig. 4A1, A2, right). The disappearance of the inhibition was already observed in the first half (5–14 days) of Dox treatment (see Supplementary Fig. 3A). Population PSTHs constructed for each mouse (Fig. 4B) evidenced that the disappearance of the inhibition was commonly observed in all 4 mice. Quantitative analysis showed that the duration and amplitude of the inhibition were markedly diminished during Dox treatment (Table 2; 1-way ANOVA with Tukey's post hoc test, $P < 0.001$ for the duration and amplitude). On the other hand, the latency, duration, and amplitude of the early excitation remained unchanged. The latency of the late excitation was decreased, and its amplitude was increased during Dox treatment ($P < 0.001$ for the duration, $P < 0.01$ for the amplitude), probably because the diminution of inhibition may unmask the late excitation. More than 15 days after the cessation of Dox treatment, a similar percentage of neurons (73%, Table 2) responded to the motor cortical stimulation, and the most common (58%) pattern was again triphasic, and was similar to that observed before Dox treatment (Fig. 4A3, left, see Supplementary Fig. 2A, After). Such recovery was also evident in population PSTHs (Fig. 4A3, right) and quantitative analyses (Table 2).

We also examined the cortically evoked responses of GPe neurons in the same 4 D1RKD mice for comparison. The most common cortically evoked response was triphasic with early excitation, followed by inhibition and late excitation throughout the 3 conditions (Fig. 4C, left; 67% before, 67% during, and 61% after Dox treatment, see Supplementary Fig. 2B); this is the typical response in WT mice (Chiken et al. 2008). In addition, population PSTHs (Fig. 4C, right) and the amplitude and duration of each component (Table 2; 1-way ANOVA; early excitation, $P = 0.51$ for the duration, $P = 0.42$ for the amplitude; inhibition, $P = 0.67$ for

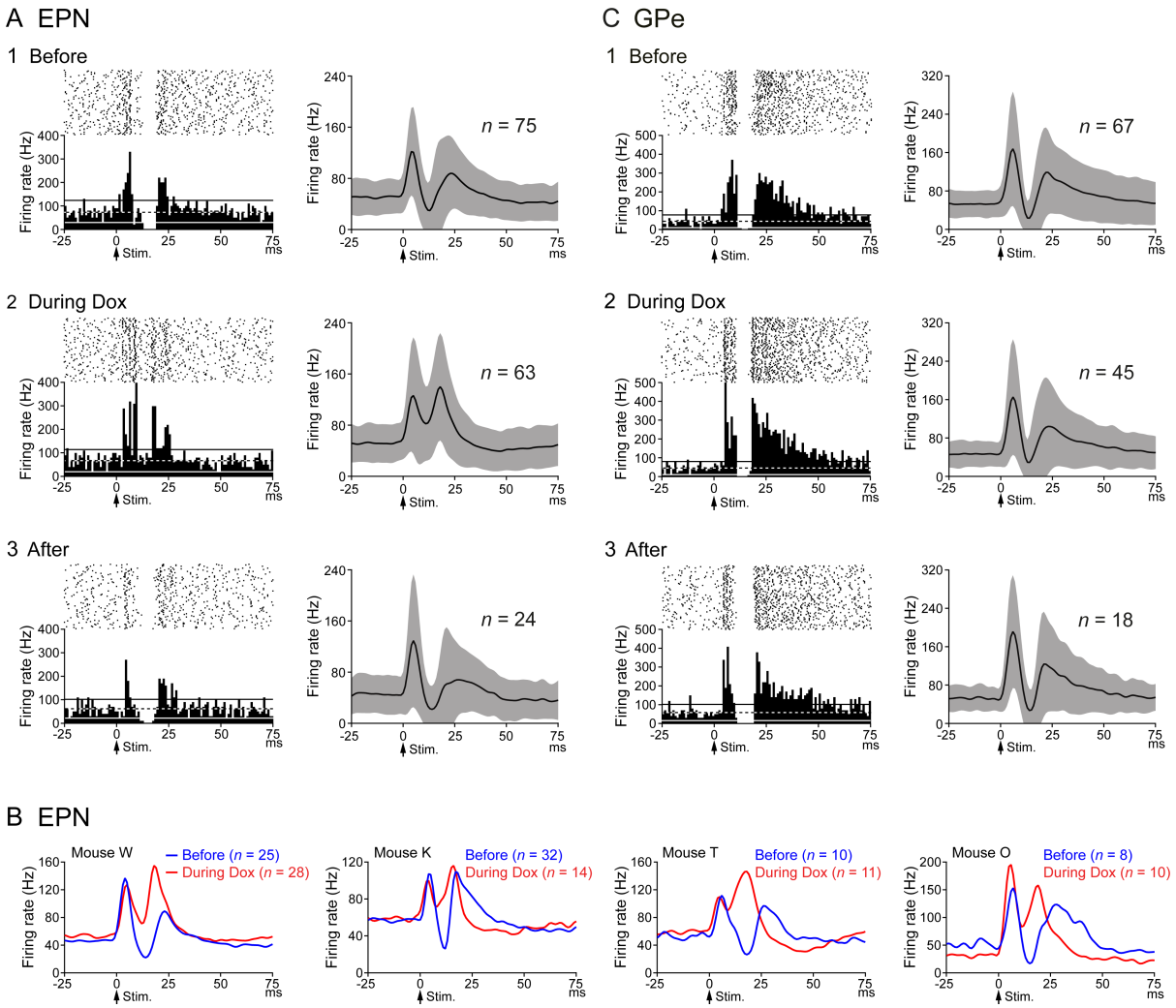


**Figure 4.** Cortically evoked responses of EPN and GPe neurons during D1R suppression. Cortically evoked responses of EPN (*A*) and GPe (*C*) neurons before (1), during (2), and after (3) Dox treatment in D1RKD mice. Raster and peristimulus time histograms (PSTHs; 100 trials; bin width, 1 ms) for typical examples (left) and population PSTHs (right, with Gaussian filter) are shown. Stimulation was delivered at time 0 (arrows). The mean firing rate and statistical levels of $P < 0.05$ (1-tailed *t*-test) are indicated in PSTHs by a black and white dashed line (mean) and black (upper limit) and white (lower limit) solid lines, respectively. The number of neurons used for population PSTHs is indicated by *n*, and the shaded areas represent ±SD. (*B*) Population PSTHs (with Gaussian filter) of cortically evoked EPN responses constructed for each mouse (mouse W, K, T, and O). Blue and red lines represent before and during Dox treatment, respectively.

the duration, $P = 0.91$ for the amplitude; late excitation, $P = 0.72$ for the duration, $P = 0.83$ for the amplitude) were similar throughout the 3 conditions.

Finally, we examined whether the effects of Dox to EPN neurons described above were specifically observed in D1RKD mice, but not in WT mice. We recorded neuronal activity in the motor-related area of the EPN in 3 age-matched WT mice before and during Dox treatment. In WT mice, Dox treatment did not change the cortically evoked response in the EPN as observed in PSTHs and population PSTHs (see Supplementary Fig. 3*B*).

### Location of Recorded Neurons

Recording sites in the EPN (mouse W) and GPe (mouse K) of D1RKD mice are shown in frontal sections using different symbols based on cortically evoked response patterns (Fig. 5). EPN neurons that responded to stimulation of the motor cortex were distributed throughout the middle and lateral parts of the EPN as observed in WT mice (Chiken et al. 2008). The most common response before Dox treatment was a triphasic response composed of early excitation, followed by inhibition and late excitation (Fig. 5*A*1). During Dox treatment, cortically evoked responses in the same area mostly changed to biphasic excitation consisting of early and late excitation (Fig. 5*A*2). GPe neurons that responded to motor cortical stimulation were distributed in the middle and lateral parts of the GPe as observed in WT mice (Chiken et al. 2008; Sano et al. 2013). The most common response was triphasic both before (Fig. 5*B*1) and during (Fig. 5*B*2) Dox treatment.

## Discussion

The present study examined motor behaviors and neuronal activity of the BG in the presence and absence of D1Rs using novel D1RKD mice that we developed in which D1R expression can be conditionally and reversibly regulated by Dox treatment. Suppression of D1R expression by Dox treatment severely

**Table 2** Cortically evoked responses of EPN and GPe neurons before, during, and after Dox treatment in D1RKD mice

| | Before | During Dox (5–22 days after starting Dox treatment) | After |
|---|---|---|---|
| EPN | | | |
| No. of responded neurons/No. of tested neurons | 75/125 (60%) | 63/88 (72%) | 24/33 (73%) |
| Early excitation | | | |
| Latency (ms) | 3.7 ± 1.0 | 3.5 ± 0.9 | 3.4 ± 0.8 |
| Duration (ms) | 3.8 ± 2.5 | 4.5 ± 2.7 | 3.8 ± 2.6 |
| Amplitude (spikes) | 43.1 ± 30.2 | 58.1 ± 54.0 | 64.7 ± 56.4 |
| Inhibition | | | |
| Latency (ms) | 11.0 ± 2.5 | 10.5 ± 2.5 | 10.3 ± 3.2 |
| Duration (ms) | 6.1 ± 5.9* | 0.8 ± 1.5*,# | 9.1 ± 6.2# |
| Amplitude (spikes) | −27.4 ± 24.4* | −3.2 ± 7.7*,# | −39.3 ± 33.9# |
| Late excitation | | | |
| Latency (ms) | 19.2 ± 3.8* | 14.1 ± 3.2*,# | 21.0 ± 5.4# |
| Duration (ms) | 7.7 ± 5.9 | 9.8 ± 6.1 | 7.1 ± 7.4 |
| Amplitude (spikes) | 54.3 ± 54.2* | 92.4 ± 79.3*,# | 51.2 ± 71.6# |
| GPe | | | |
| No. of responded neurons/No. of tested neurons | 67/114 (59%) | 45/82 (55%) | 18/30 (60%) |
| Early excitation | | | |
| Latency (ms) | 3.9 ± 1.3 | 4.1 ± 1.0 | 4.0 ± 1.4 |
| Duration (ms) | 5.4 ± 2.7 | 6.0 ± 3.5 | 5.9 ± 1.9 |
| Amplitude (spikes) | 80.5 ± 48.7 | 83.5 ± 40.7 | 96.3 ± 42.8 |
| Inhibition | | | |
| Latency (ms) | 10.8 ± 2.4 | 11.2 ± 2.6 | 11.8 ± 1.9 |
| Duration (ms) | 6.1 ± 5.4 | 7.3 ± 6.7 | 6.6 ± 10.6 |
| Amplitude (spikes) | −31.8 ± 30.6 | −32.3 ± 24.9 | −36.0 ± 74.7 |
| Late excitation | | | |
| Latency (ms) | 20.2 ± 4.2 | 19.9 ± 4.0 | 19.8 ± 3.8 |
| Duration (ms) | 21.6 ± 36.0 | 17.2 ± 25.1 | 17.5 ± 16.5 |
| Amplitude (spikes) | 196.1 ± 392.0 | 159.5 ± 292.7 | 162.5 ± 177.6 |

*,#$P < 0.01$, significantly different from each other (1-way ANOVA with Tukey's post hoc test).

impaired motor behaviors in the mice. Cortically evoked inhibition in the EPN, which is mediated by the cortico-striato-EPN direct pathway, was mostly lost during suppression of D1R expression, whereas spontaneous firing rates and patterns of EPN neurons remained unchanged. These results suggest that D1R-mediated dopaminergic transmission maintains the information flow through the cortico-striato-EPN direct pathway to appropriately release motor actions.

## Motor Behaviors and Spontaneous Activity of EPN and GPe Neurons

Based on the classical model of the BG, dopaminergic inputs exert excitatory effects on striatal direct pathway neurons through D1Rs (Albin et al. 1989; DeLong 1990; Gerfen et al. 1990). Thus, the loss of dopaminergic inputs through D1Rs would be expected to increase mean firing of EPN neurons and result in decreased motor activity. Increased mean firing rates were originally reported in the GPi (EPN in rodents) of primate models of PD (Miller and DeLong 1987; Filion and Tremblay 1991; Boraud et al. 1998; Heimer et al. 2002; Wichmann et al. 2002). However, recent studies have failed to detect the expected firing rate increase in the GPi (Wichmann et al. 1999; Raz et al. 2000; Tachibana et al. 2011). Instead, abnormal firing patterns, such as bursts and oscillations, were recorded in the BG of PD animals and patients (Raz et al. 2000; Brown et al. 2001; Tachibana et al. 2011), and synchronous activation may disable the ability of individual neurons to process and relay motor-related information, resulting in failure of appropriate movements (Bergman et al. 1998; Brown 2007). The present study revealed that spontaneous motor activity in the mice was decreased during suppression of D1R expression (Fig. 2) without any prominent effects on spontaneous firing rates in either the EPN or GPe (Table 1, Fig. 3). The results indicate that the motor deficits during the absence of D1R-mediated dopaminergic transmission cannot be explained simply by changes in spontaneous firing rates in the EPN.

## Cortically Evoked Responses of EPN and GPe Neurons

The BG receive inputs from a wide area of the cerebral cortex (Mink 1996; Nambu et al. 2002). The information is processed through the cortico-STN-EPN hyperdirect, cortico-striato-EPN direct, and cortico-striato-GPe-STN-EPN indirect pathways and reaches the EPN, the output station of the BG (Fig. 1A). During voluntary movements, neuronal signals originating in the cortex are considered to be transmitted through these pathways and reach the EPN. Thus, evaluating how neuronal signals originating in the motor cortex are transmitted through the BG is essential for assessing the mechanism of abnormal motor behaviors. Cortical stimulation induces neuronal activity in the BG mimicking information processing during voluntary movements and providing important clues for understanding the changes in information processing through the BG (Chiken et al. 2008; Tachibana et al. 2008; Sano et al. 2013). Cortically evoked responses in the BG are dramatically altered in hyper- and hypokinetic movement disorders (Chiken et al. 2008; Kita and Kita 2011; Nishibayashi et al. 2011).

Before Dox treatment, cortical stimulation induced a triphasic response composed of early excitation, followed by inhibition and late excitation in the EPN of D1RKD mice (Fig. 4A1); this is the typical response in WT mice (Chiken et al. 2008, see Supplementary Fig. 3B). D1RKD mice also showed normal behaviors and similar spontaneous motor activity to WT mice despite a high level of D1R expression, suggesting compensatory mechanisms, such as desensitization of D1Rs (Staunton et al. 1982) and decrease of dopamine release. Transient increase of spontaneous motor activity after cessation of Dox treatment (Fig. 2C) also suggests involvement of compensatory mechanisms, such as sensitization of D1Rs and increase of dopamine release. During suppression of D1R expression, cortically evoked inhibition in the EPN was mostly lost (Fig. 4A2, Table 2, see Supplementary Fig. 2A). On the other hand, cortical stimulation induced a triphasic response composed of early excitation, followed by inhibition and late excitation in the GPe that was not changed during D1R suppression (Fig. 4C, Table 2, see Supplementary Fig. 2B).

Many studies have revealed that cortically evoked early excitation, inhibition, and late excitation in the EPN/GPi are mediated by the hyperdirect, direct, and indirect pathways, respectively (Maurice et al. 1999; Nambu et al. 2000, 2002; Tachibana et al.

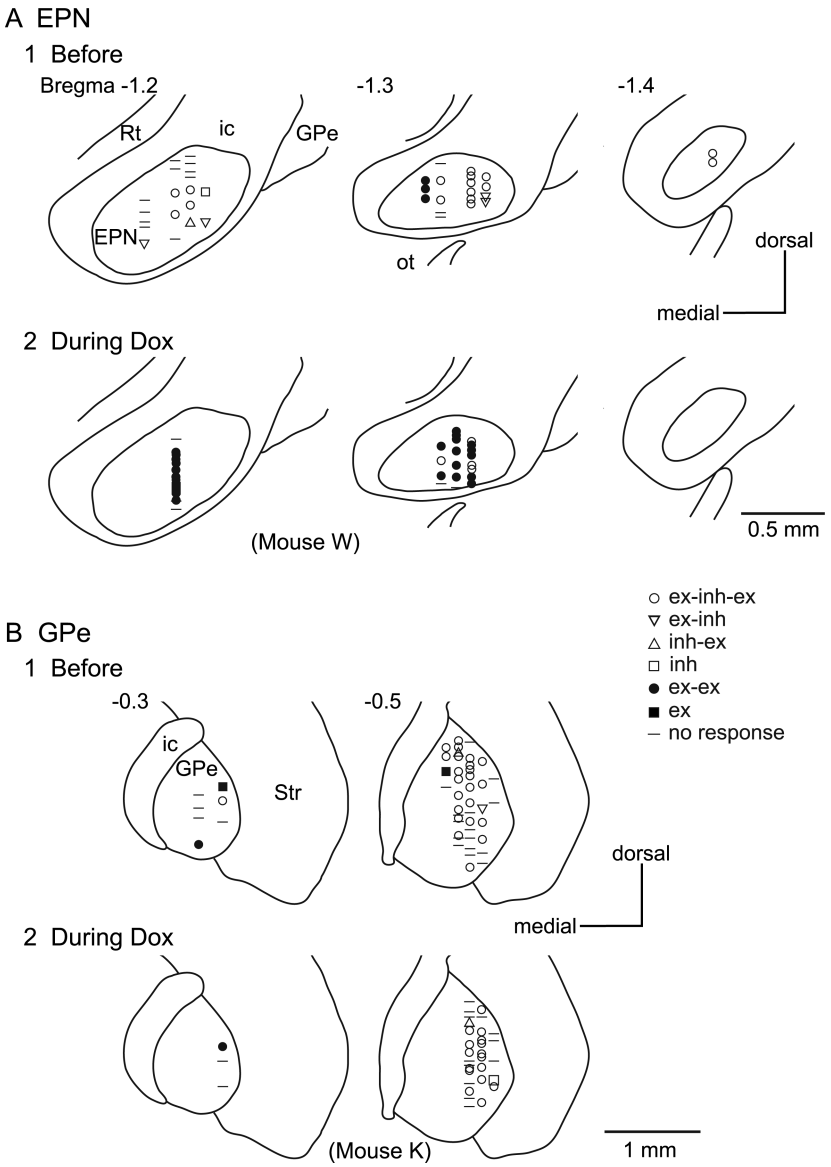


**Figure 5.** Recording sites in the EPN (*A*) (Mouse W) and GPe (*B*) (Mouse K) of D1RKD mice before (*1*) and during (*2*) Dox treatment. Frontal sections are arranged rostrocaudally from left to right, and the distance from bregma to each section is indicated. Locations of recorded neurons are indicated by different symbols based on cortically evoked response patterns. ex, excitation; ic, internal capsule; inh, inhibition; ot, optic tract; Rt, reticular thalamic nucleus; Str, striatum.

2008) (Fig. 1A). Thus, the loss of inhibition in the EPN during D1R suppression indicates that information flow through the cortico-striato-EPN direct pathway was strongly suppressed. Several possible mechanisms for this suppression can be considered. First, the excitability of striatal direct pathway neurons may be decreased during D1R suppression. The heads of dendritic spines of striatal projection neurons receive excitatory inputs from cortical neurons, with the neck of the spine receiving dopaminergic inputs through synapses and/or volume transmission (Hersch et al. 1995; Smith and Kieval 2000; Arbuthnott and Wickens 2007). This spatial arrangement allows dopamine to modulate incoming excitatory glutamatergic drive. D1Rs are coupled to $G_{s/olf}$, which activates adenylyl cyclase and facilitates intrinsic excitability and glutamate receptor-mediated responses in striatal neurons (Hervé et al. 1995; Surmeier et al. 2007; Gerfen and Surmeier 2011). D1R activation increases synaptic efficacy in cortico-striatal synapses through long-term potentiation (Calabresi et al. 2007; Gerfen and Surmeier 2011). A significant loss of dendritic spines on striatal projection neurons in PD has also been reported (Villalba and Smith 2010). Second, other extrastriatal mechanisms can also be considered. A previous study (Kliem et al. 2007) revealed that D1Rs are also expressed in striatal axon terminals in the GPi, and their activation increases GABA release from the striato-GPi axon terminals. Decreased GABA release from the striato-EPN (homologous to GPi) terminals may contribute to loss of cortically evoked inhibition in the EPN. The EPN also receives GABAergic inhibitory inputs from the GPe. However, considering the fact that both spontaneous firing and the cortically evoked response in the GPe remained unchanged during D1R suppression (Fig. 3B, Fig. 4C, Tables 1 and 2, see Supplementary Fig. 2B), the GPe cannot be responsible for the attenuated cortically evoked inhibition in the EPN.

The cortically evoked triphasic response in the GPe is mediated sequentially by the cortico-STN-GPe, cortico-striato-GPe, and cortico-striato-GPe-STN-GPe pathways (Maurice et al. 1999; Nambu et al. 2000, 2002; Kita et al. 2004) (Fig. 1A). The maintained triphasic response in the GPe in the absence of D1Rs (Fig. 4C, Table 2, see Supplementary Fig. 2B) suggests that the excitability of these components, including the cortex, striatal indirect pathway neurons, GPe, and STN, remains unchanged despite the fact that D1Rs are also expressed at moderate levels in the cortex (Fig. 1C; Fremeau et al. 1991; Weiner et al. 1991; Gaspar et al. 1995). In situ hybridization study using a D2R-specific riboprobe followed by immunohistochemistry with Cre-specific antibody indicated that D1Rs may also be aberrantly expressed in striato-GPe indirect pathway neurons in transgenic mice expressing a Cre recombinase under the control of the D1R regulatory elements (Lemberger et al. 2007). However, neither spontaneous discharges nor cortically evoked responses of GPe neurons changed during D1R suppression in our current electrophysiological study (Figs 3B and 4C, Tables 1 and 2, see Supplementary Fig. 2B), suggesting that they are less functional.

Recent studies have shown conflicting results regarding the classical direct and indirect pathways model. Striatal neurons projecting to the EPN also have axon collaterals to the GPe, indicating no clear anatomical separation of the direct and indirect pathways (Graybiel 2005; Lévesque and Parent 2005; Fujiyama et al. 2011). Some striatal projection neurons express both D1Rs and D2Rs (Surmeier et al. 1996). However, the present results support the original notion that striatal projection neurons can be functionally separated into 2 groups, that is, one with D1Rs projecting to the EPN (GPi) and the other with D2Rs projecting to the GPe (Albin et al. 1989; DeLong 1990; Gerfen et al. 1990; Hersch et al. 1995; Sano et al. 2013). The axon terminals of striatal neurons that express D1Rs in the GPe may be minor or less functional compared with those with D2Rs.

### D1R-Mediated Dopaminergic Transmission Maintains the Information Flow Through the Direct Pathway to Release Motor Actions

During D1R suppression, cortically evoked inhibition in the EPN was mostly lost (Fig. 4A,B), and motor behaviors were severely impaired (Fig. 2). Upon D1R re-expression, both the inhibition and motor behaviors were restored. This observation can explain the mechanism of reduced motor activity during D1R suppression (see Supplementary Fig. 4). Under normal D1R expression (see Supplementary Fig. 4, left), signals through the cortico-striato-EPN direct pathway induce inhibition in the EPN. The phasic inhibition in the EPN increases thalamocortical activity by disinhibitory mechanism and releases motor actions (Albin et al. 1989; DeLong 1990; Gerfen et al. 1990; Mink 1996; Hikosaka et al. 2000; Nambu et al. 2000, 2002; Nambu 2007; Kravitz et al. 2010). During D1R suppression (see Supplementary Fig. 4, right), signals through the cortico-striato-EPN direct pathway are strongly suppressed and fail to induce inhibition in the EPN, resulting in the reduced motor activity. Moreover, this observation suggests that the loss of the phasic inhibition in the EPN through the direct pathway, but not the firing rate or pattern changes, is a fundamental phenomenon in reduced motor activity during D1R suppression. The reduction of spontaneous motor activity was observed even in the first week of Dox treatment (Fig. 2A) when the level of D1R expression was still higher than that in WT mice (Fig. 1D). The loss of cortically evoked inhibition in EPN neurons was already observed in the first half (5–14 days) of Dox treatment (see Supplementary Fig. 3A). These results suggest that relative decrease of D1R expression would be responsible for the changes in motor behavior and neuronal activity. Considering the fact that expression of D1Rs not only in the striatum but also outside the striatum was suppressed during Dox treatment in D1RKD mice (Fig. 1C), we cannot rule out the possibility that loss of extrastriatal D1Rs were also involved in their behavioral changes observed in the current study.

The present study revealed a crucial role for dopamine in maintaining the dynamics of the BG circuitry: D1R-mediated dopaminergic transmission maintains the information flow through the cortico-striato-EPN (GPi) direct pathway to appropriately release motor actions through disinhibitory mechanisms (see Supplementary Fig. 4). The present results also suggest that phasic activity changes in the EPN through the cortico-striato-EPN direct pathway are fundamental to both normal functions of the BG and the pathophysiology of movement disorders. Dopamine deficiency impairs phasic activation of the cortico-striato-EPN direct pathway and release of motor actions, and would be involved in the bradykinesia seen in PD.

## Supplementary Material

Supplementary material can be found at: http://www.cercor.oxfordjournals.org/.

## Funding

This study was supported by JSPS KAKENHI (#23115721, #21500378 and #25430021 to S.C.), JSPS KAKENHI (#22500343 and #26290029), the Collaborative Research Project (#2011-2221) of Brain Research Institute, Niigata University and the MEXT-Supported Program for the Strategic Research Foundation at Private Universities, 2011-2015 (to T.S.), and JSPS KAKENHI (#21240039, #26250009 and #15H05873), CREST, Strategic Japanese-German Cooperative Programme and the Takeda Science Foundation (to A.N.). Funding to pay the Open Access publication charges for this article was provided by the JSPS KAKENHI (#15H05873).

## Notes

We thank M. Katsuki, A. Aiba, K. Nakamura, and K. Nakao for technical advice and critical discussion on generation of the D1RKD mice, K. Miyamoto, S. Sato, K. Awamura, H. Isogai, M. Goto, and members of the Department of Comparative and Experimental Medicine, Brain Research Institute, Niigata University for technical assistance. We also thank M. Kimura, Y. Kubo, and Y. Yamagata for comments on the manuscript. *Conflict of Interest*: None declared.

## References

Albin RL, Young AB, Penney JB. 1989. The functional anatomy of basal ganglia disorders. Trends Neurosci. 12:366–375.

Arbuthnott GW, Wickens J. 2007. Space, time and dopamine. Trends Neurosci. 30:62–69.

Bergman H, Feingold A, Nini A, Raz A, Slovin H, Abeles M, Vaadia E. 1998. Physiological aspects of information processing in the basal ganglia of normal and parkinsonian primates. Trends Neurosci. 21:32–38.

Boraud T, Bezard E, Guehl D, Bioulac B, Gross C. 1998. Effects of L-DOPA on neuronal activity of the globus pallidus externalis (GPe) and globus pallidus internalis (GPi) in the MPTP-treated monkey. Brain Res. 787:157–160.

Brown P. 2007. Abnormal oscillatory synchronisation in the motor system leads to impaired movement. Curr Opin Neurobiol. 17:656–664.

Brown P, Oliviero A, Mazzone P, Insola A, Tonali P, Di Lazzaro V. 2001. Dopamine dependency of oscillations between subthalamic nucleus and pallidum in Parkinson's disease. J Neurosci. 21:1033–1038.

Calabresi P, Picconi B, Tozzi A, Di Filippo M. 2007. Dopamine-mediated regulation of corticostriatal synaptic plasticity. Trends Neurosci. 30:211–219.

Chiken S, Shashidharan P, Nambu A. 2008. Cortically evoked long-lasting inhibition of pallidal neurons in a transgenic mouse model of dystonia. J Neurosci. 28:13967–13977.

Day M, Wokosin D, Plotkin JL, Tian X, Surmeier DJ. 2008. Differential excitability and modulation of striatal medium spiny neuron dendrites. J Neurosci. 28:11603–11614.

DeLong MR. 1990. Primate models of movement disorders of basal ganglia origin. Trends Neurosci. 13:281–285.

Enomoto K, Matsumoto N, Nakai S, Satoh T, Sato TK, Ueda Y, Inokawa H, Haruno M, Kimura M. 2011. Dopamine neurons learn to encode the long-term value of multiple future rewards. Proc Natl Acad Sci USA. 108:15462–15467.

Fahn S, Jankovic J, Hallett M. 2011. Principles and practice of movement disorders. 2nd ed. Philadelphia: Elsevier Saunders.

Filion M, Tremblay L. 1991. Abnormal spontaneous activity of globus pallidus neurons in monkeys with MPTP-induced parkinsonism. Brain Res. 547:142–151.

Flores-Barrera E, Vizcarra-Chacon BJ, Bargas J, Tapia D, Galarraga E. 2011. Dopaminergic modulation of corticostriatal responses in medium spiny projection neurons from direct and indirect pathways. Front Syst Neurosci. 5:15.

Fremeau RT Jr, Duncan GE, Fornaretto MG, Dearry A, Gingrich JA, Breese GR, Caron MG. 1991. Localization of D1 dopamine receptor mRNA in brain supports a role in cognitive, affective, and neuroendocrine aspects of dopaminergic neurotransmission. Proc Natl Acad Sci USA. 88:3772–3776.

Fujiyama F, Sohn J, Nakano T, Furuta T, Nakamura KC, Matsuda W, Kaneko T. 2011. Exclusive and common targets of neostriatofugal projections of rat striosome neurons: a single neuron-tracing study using a viral vector. Eur J Neurosci. 33:668–677.

Gaspar P, Bloch B, Le Moine C. 1995. D1 and D2 receptor gene expression in the rat frontal cortex: cellular localization in different classes of efferent neurons. Eur J Neurosci. 7:1050–1063.

Gerfen CR, Engber TM, Mahan LC, Susel Z, Chase TN, Monsma FJ Jr, Sibley DR. 1990. D1 and D2 dopamine receptor-regulated gene expression of striatonigral and striatopallidal neurons. Science. 250:1429–1432.

Gerfen CR, Surmeier DJ. 2011. Modulation of striatal projection systems by dopamine. Annu Rev Neurosci. 34:441–466.

Graybiel AM. 2005. The basal ganglia: learning new tricks and loving it. Curr Opin Neurobiol. 5:638–644.

Heimer G, Bar-Gad I, Goldberg JA, Bergman H. 2002. Dopamine replacement therapy reverses abnormal synchronization of pallidal neurons in the 1-methyl-4-phenyl-1,2,3,6-tetrahydropyridine primate model of parkinsonism. J Neurosci. 22:7850–7855.

Hersch SM, Ciliax BJ, Gutekunst CA, Rees HD, Heilman CJ, Yung KK, Bolam JP, Ince E, Yi H, Levey AI. 1995. Electron microscopic analysis of D1 and D2 dopamine receptor proteins in the dorsal striatum and their synaptic relationships with motor corticostriatal afferents. J Neurosci. 15:5222–5237.

Hervé D, Rogard M, Lévi-Strauss M. 1995. Molecular ananysis of the multiple Golf alpha subunit mRNAs in the rat brain. Brain Res Mol Brain Res. 32:125–134.

Hikosaka O, Takikawa Y, Kawagoe R. 2000. Role of the basal ganglia in the control of purposive saccadic eye movements. Physiol Rev. 80:953–978.

Hirsch EC, Périer C, Orieux G, François C, Féger J, Yelnik J, Vila M, Levy R, Tolosa ES, Marin C, et al. 2000. Metabolic effects of nigrostriatal denervation in basal ganglia. Trends Neurosci. 23: S78–S85.

Hutchison WD, Allan RJ, Opitz H, Levy R, Dostrovsky JO, Lang AE, Lozano AM. 1998. Neurophysiological identification of the subthalamic nucleus in surgery for Parkinson's disease. Ann Neurol. 44:622–628.

Joshua M, Adler A, Bergman H. 2009. The dynamics of dopamine in control of motor behavior. Curr Opin Neurobiol. 19:615–620.

Kita H, Nambu A, Kaneda K, Tachibana Y, Takada M. 2004. Role of ionotropic glutamatergic and GABAergic inputs on the firing activity of neurons in the external pallidum in awake monkeys. J Neurophysiol. 92:3069–3084.

Kita T, Kita H. 2011. Cortical stimulation evokes abnormal responses in the dopamine-depleted rat basal ganglia. J Neurosci. 31:10311–10322.

Kliem MA, Maidment NT, Ackerson LC, Chen S, Smith Y, Wichmann T. 2007. Activation of nigral and pallidal dopamine D1-like receptors modulates basal ganglia outflow in monkeys. J Neurophysiol. 98:1489–1500.

Kravitz AV, Freeze BS, Parker PR, Kay K, Thwin MT, Deisseroth K, Kreitzer AC. 2010. Regulation of parkinsonian motor behaviours by optogenetic control of basal ganglia circuitry. Nature. 466:622–626.

Legéndy CR, Salcman M. 1985. Bursts and recurrences of bursts in the spike trains of spontaneously active striate cortex neurons. J Neurophysiol. 53:926–939.

Lemberger T, Parlato R, Dassesse D, Westphal M, Casanova E, Turiault M, Tronche F, Schiffmann SN, Schutz G. 2007. Expression of Cre recombinase in dopaminoceptive neurons. BMC Neuroscience. 8:4.

Lévesque M, Parent A. 2005. The striatofugal fiber system in primates: a reevaluation of its organization based on single-axon tracing studies. Proc Natl Acad Sci USA. 102:11888–11893.

Mallet N, Ballion B, Le Moine C, Gonon F. 2006. Cortical inputs and GABA interneurons imbalance projection neurons in the striatum of parkinsonian rats. J Neurosci. 26:3875–3884.

Maurice N, Deniau JM, Glowinski J, Thierry AM. 1999. Relationships between the prefrontal cortex and the basal ganglia in the rat: physiology of the cortico-nigral circuits. J Neurosci. 19:4674–4681.

Miller WC, DeLong MR. 1987. Altered tonic activity of neurons in the globus pallidus and subthalamic nucleus in the primate MPTP model of parkinsonism. In: Carpenter MB, Jayaraman A, editors. The basal ganglia II: structure and functions-current concepts. New York: Plenum. p. 415–427.

Mink JW. 1996. The basal ganglia: focused selection and inhibition of competing motor programs. Prog Neurobiol. 50:381–425.

Nagy A, Gertsenstein M, Vintersten K, Behringer R. 2002. Manipulating the mouse embryo: a laboratory manual. 3rd ed. New York: Cold Spring Harbor Press.

Nakamura T, Sato A, Kitsukawa T, Momiyama T, Yamamori T, Sasaoka T. 2014. Distinct motor impairments of dopamine D1 and D2 receptor knockout mice revealed by three types of motor behavior. Front Integr Neurosci. 8:56.

Nambu A. 2007. Globus pallidus internal segment. Prog Brain Res. 160:135–150.

Nambu A, Tokuno H, Hamada I, Kita H, Imanishi M, Akazawa T, Ikeuchi Y, Hasegawa N. 2000. Excitatory cortical inputs to pallidal neurons via the subthalamic nucleus in the monkey. J Neurophysiol. 84:289–300.

Nambu A, Tokuno H, Takada M. 2002. Functional significance of the cortico-subthalamo-pallidal 'hyperdirect' pathway. Neurosci Res. 43:111–117.

Nishibayashi H, Ogura M, Kakishita K, Tanaka S, Tachibana Y, Nambu A, Kita H, Itakura T. 2011. Cortically evoked responses of human pallidal neurons recorded during stereotactic neurosurgery. Mov Disord. 26:469–476.

Planert H, Berger TK, Silberberg G. 2013. Membrane properties of striatal direct and indirect pathway neurons in mouse and rat slices and their modulation by dopamine. PLoS One. 8:e57054.

Raz A, Vaadia E, Bergman H. 2000. Firing patterns and correlations of spontaneous discharge of pallidal neurons in the normal and the tremulous 1-methyl-4-phenyl-1,2,3,6-tetrahydropyridine vervet model of parkinsonism. J Neurosci. 20:8559–8571.

Sano H, Chiken S, Hikida T, Kobayashi K, Nambu A. 2013. Signals through the striatopallidal indirect pathway stop movements by phasic excitation in the substantia nigra. J Neurosci. 33:7586–7594.

Seppi K, Weintraub D, Coelho M, Perez-Lloret S, Fox SH, Katzenschlager R, Hametner EM, Poewe W, Rascol O, Goetz CG, et al. 2011. The movement disorder society evidence-based medicine review update: treatments for the non-motor symptoms of Parkinson's disease. Mov Disord. 26 Suppl 3:S42–S80.

Smith Y, Kieval JZ. 2000. Anatomy of the dopamine system in the basal ganglia. Trends Neurosci. 23:S28–S33.

Staunton DA, Magistretti PJ, Koob GF, Shoemaker WJ, Bloom FE. 1982. Dopaminergic supersensitivity induced by denervation and chronic receptor blockade is additive. Nature. 299:72–74.

Surmeier DJ, Ding J, Day M, Wang Z, Shen W. 2007. D1 and D2 dopamine-receptor modulation of striatal glutamatergic signaling in striatal medium spiny neurons. Trends Neurosci. 30:228–235.

Surmeier DJ, Song WJ, Yan Z. 1996. Coordinated expression of dopamine receptors in neostriatal medium spiny neurons. J Neurosci. 16:6579–6591.

Tachibana Y, Iwamuro H, Kita H, Takada M, Nambu A. 2011. Subthalamo-pallidal interactions underlying parkinsonian neuronal oscillations in the primate basal ganglia. Eur J Neurosci. 34:1470–1484.

Tachibana Y, Kita H, Chiken S, Takada M, Nambu A. 2008. Motor cortical control of internal pallidal activity through glutamatergic and GABAergic inputs in awake monkeys. Eur J Neurosci. 27:238–253.

Tran AH, Uwano T, Kimura T, Hori E, Katsuki M, Nishijo H, Ono T. 2008. Dopamine D1 receptor modulates hippocampal representation plasticity to spatial novelty. J Neurosci. 28: 13390–13400.

Villalba RM, Smith Y. 2010. Striatal spine plasticity in Parkinson's disease. Front Neuroanat. 4:133.

Waddington JL, O'Tuathaigh C, O'Sullivan G, Tomiyama K, Koshikawa N, Croke DT. 2005. Phenotypic studies on dopamine receptor subtype and associated signal transduction mutants: insights and challenges from 10 years at the psychopharmacology-molecular biology interface. Psychopharmacology. 181:611–638.

Weiner DM, Levey AI, Sunahara RK, Niznik HB, O'Dowd BF, Seeman P, Brann MR. 1991. D1 and D2 dopamine receptor mRNA in rat brain. Proc Natl Acad Sci USA. 88:1859–1863.

Wichmann T, Bergman H, Starr PA, Subramanian T, Watts RL, DeLong MR. 1999. Comparison of MPTP-induced changes in spontaneous neuronal discharge in the internal pallidal segment and in the substantia nigra pars reticulata in primates. Exp Brain Res. 125:397–409.

Wichmann T, Kliem MA, Soares J. 2002. Slow oscillatory discharge in the primate basal ganglia. J Neurophysiol. 87: 1145–1148.

Yang XW, Model P, Heintz N. 1997. Homologous recombination based modification in *Escherichia coli* and germline transmission in transgenic mice of a bacterial artificial chromosome. Nat Biotechnol. 15:859–865.